Ruthenium(II) 1,4,7-trithiacyclononane complexes of curcumin and bisdemethoxycurcumin: Synthesis, characterization, and biological activity

Riccardo Pettinari [a,*], Fabio Marchetti [b], Alessia Tombesi [b], Fenghe Duan [a], Liming Zhou [c], Luigi Messori [d], Chiara Giacomelli [e], Laura Marchetti [e], Maria Letizia Trincavelli [e], Tiziano Marzo [e], Diego La Mendola [e], Gabriele Balducci [f], Enzo Alessio [f,*]

[a] *School of Pharmacy, University of Camerino, Via S. Agostino 1, 62032 Camerino, MC, Italy*
[b] *School of Science and Technology, University of Camerino, Via S. Agostino 1, 62032 Camerino, MC, Italy*
[c] *Henan Provincial Key Laboratory of Surface and Interface Science, Zhengzhou University of Light Industry, Zhengzhou, 450002, PR China*
[d] *Department of Chemistry, University of Florence, Via della Lastruccia 3-13, Sesto Fiorentino, Florence, Italy*
[e] *Department of Pharmacy, University of Pisa, Via Bonanno Pisano, 6, 56126, Pisa, Italy*
[f] *Department of Chemical and Pharmaceutical Sciences, University of Trieste, Via L. Giorgieri 1, Trieste, Italy*

A R T I C L E I N F O

Keywords:
Curcumin
Bisdemethoxycurcumin
Ruthenium complexes
1,4,7-trithiacyclononane
Anticancer activity
Metal complexes interaction with protein lysozyme

A B S T R A C T

Two cationic ruthenium(II) 1,4,7-trithiacyclononane ([9]aneS_3) complexes of curcumin (curcH) and bisdemethoxycurcumin (bdcurcH), namely [Ru(curc)(dmso-S)([9]aneS_3)]Cl (**1**) and [Ru(bdcurc)(dmso-S)([9]aneS_3)]Cl (**2**) were prepared from the [RuCl_2(dmso-S)([9]-aneS_3)] precursor and structurally characterized, both in solution and in the solid state by X-ray crystallography. The corresponding PTA complexes [Ru(curc)(PTA)([9]aneS_3)]Cl (**3**) and [Ru(bdcurc)(PTA)([9]aneS_3)]Cl (**4**) have been also synthesized and characterized (PTA = 1,3,5-triaza-7-phosphaadamantane). Bioinorganic studies relying on mass spectrometry were performed on complexes **1**–**4** to assess their interactions with the model protein lysozyme. Overall, a rather limited reactivity with lysozyme was highlighted accompanied by a modest cytotoxic potency against three representative cancer cell lines. The moderate pharmacological activity is likely connected to the relatively high stability of these complexes.

1. Introduction

Curcumin (curcH) is the major component of the Oriental spice turmeric, obtained from the rhizome of the *Curcuma longa* [1]. The medicinal properties of curcumin are well known due to its antioxidant, anti-inflammatory, antimicrobial, and anticancer actions [2].

One of the major problems faced in clinical trials involving curcumin is its poor solubility and absorption, high metabolic rate and fast systemic elimination from the body, leading to low levels in plasma and tissues [3]. One way to increase the bioavailability of curcumin could be to synthesize metal complexes with higher solubility than free curcumin [4,5]. Metal complexes containing curcumin can be classified into two distinct groups. The first one is represented by homoleptic complexes, in which two or three deprotonated curcumins are coordinated to the metal center [6]. The second group comprises heteroleptic complexes where a deprotonated curcumin and co-ligands are coordinated to the metal center [6]. Although the number of works on curcumin metal complexes is very large, the crystal structures of these complexes are scarce. To our knowledge, none of the homoleptic curcumin complexes has been structurally authenticated by X-ray diffraction and only few heteroleptic complexes have been structurally characterized. Suitable co-ligands to complete the coordination enviroment of the metal ions in addition to curcumin include 2,2-bipyridine [7], [8] 1,10-phenanthroline [7], terpyridine [9], [10] tertiary phosphines [11], pentamethylcyclopentadienyl [12], or arene ligands (arene = *p*-cymene [13–15], hexamethlybenzene [14] and 2-phenylethan-1-ol [16]). Some half-sandwich Ru(II) complexes display much bigger antiproliferative activity with respect to platinum complexes [17–19], in particular complexes with curcumin and bisdemethoxycurcumin are very cytotoxic and, interestingly, the combination of the curcuminoids with PTA (1,3,5-triaza-7-phosphaadamantane) produced the most cytotoxic compounds for several tested cell lines with a potency comparable to cisplatin [14]. Comparative investigations of in vivo interactions between RAPTA-complexes with curcuminoid ligands and human serum

* Corresponding authors.
E-mail address: riccardo.pettinari@unicam.it (R. Pettinari).

Accepted 2 February 2021

albumin [20] or ct-DNA [21] were recently reported.

1,4,7-trithiacyclononane ([9]aneS_3) is a neutral face-capping ligand that has been proposed as a possible alternative for the η^6-arene fragment. Several Ru(II)-[9]aneS_3 compounds have been investigated as potential cytotoxic agents [22–24]. [25–27] Recently, Braga and coworkers reported the synthesis of [([9]aneS_3)(curc)(dmso-S)Ru]Cl, and determined its in vitro cytotoxic activity against human prostate cancer cell line (PC-3) and healthy cell line (PNT-2). Nevertheless, the X-ray structure of such compound was not obtained [28]. Here we describe the synthesis and characterization of Ru(II)-[9]aneS_3 complexes with curcumin and bisdemethoxycurcumin proligands, and their PTA-containing counterparts. In this work we have been able to obtain, for the first time, the X-ray structure of two ruthenium curcumin complexes containing the [9]aneS_3 co-ligand. Additionally, ESI-MS experiments were carried out to characterize the reactivity of the study complexes toward a model protein target i.e. hen egg white lysozyme (HEWL). Biological tests were also performed to assess the cytotoxic potency of these compounds against three reference cancer cell lines i.e. A549, adenocarcinoma human alveolar basal epithelial cells (NSCLC); MCF7, breast cancer cell line (ER+, PR+, HER2-) and HCT116, colorectal cancer cell line. Altogether, results reveal a rather low reactivity of the four complexes when challenged with HEWL, that seems to be consistent with their modest cytotoxic activity. Advantages and disadvantages inherent to this biological behavior are discussed.

2. Results and discussion

2.1. Synthesis and characterization

[Ru(curc)(dmso-S)([9]aneS_3)]Cl (**1**) and [Ru(bdcurc)(dmso-S)([9]aneS_3)]Cl (**2**) were prepared in moderate yield by reacting [RuCl_2(dmso-S)([9]aneS_3)] and the curcH and bdcurcH proligands in methanol with potassium hydroxide as deprotonating agent (Scheme 1). Compounds **1** and **2** are air-stable in the solid-state and in solution; they are soluble in most organic solvents and also in water (the solubility values are reported in Table S3). They were characterized by elemental analysis, infrared, UV–Visible, ^{1}H and ^{13}C{^{1}H} NMR spectroscopy and ESI mass spectrometry.

In acetonitrile and DMSO they display conductivity values within the range typical for a 1:1 electrolyte. In the IR spectra of **1–2** the shift of the ν(C=O) absorption bands of the curcuminoid ligand to lower wavenumbers confirms coordination to the ruthenium(II) center in the O,O′-bidentate chelating mode. The ESI mass spectra of **1**–**2** in positive ion mode provide peaks corresponding to cation fragments [Ru(curc)(dmso-S)([9]aneS_3)]$^+$ and [Ru(bdcurc)(dmso-S)([9]aneS_3)]$^+$, respectively The ^{1}H and ^{13}C{^{1}H} NMR spectra of **1**–**2** recorded in DMSO-d_6 contain a set of signals for the resonances of the curcuminoid ligands, with the expected shifts in frequency in comparison to the free proligands. The proton and carbon assignments were made based on previous studies on analogous complexes. Reaction of **1**–**2** with the water-soluble phosphine PTA in acetone afforded the corresponding complexes [Ru(curc)(PTA)([9]aneS_3)]Cl (**3**) and [Ru(bdcurc)(PTA)([9]aneS_3)]Cl (**4**) upon selective replacement of the dmso-S ligand by PTA (Scheme 2). Complexes **3** and **4** are soluble in most organic solvents and are very soluble also in water (the solubility values are reported in Table S3). In acetonitrile and DMSO they display conductivity values within the range typical for 1:1 electrolytes. The ^{1}H NMR spectra of **3** and **4** show the expected signals due to the coordinated [9]aneS_3, curcuminoids, and PTA ligands. Additionally, in the ^{31}P{^{1}H} NMR spectra of **3** and **4**, the phosphorus of PTA affords singlets at −28.7 ppm, which are consistent with previous reports [29]. The positive ion ESI mass spectra of **3** and **4** contain ions corresponding to the species [Ru(curc)(PTA)([9]aneS_3)]$^+$ and [Ru(bdcurc)(PTA)([9]aneS_3)]$^+$, respectively.

The stability of Ru(II) complexes was also studied: in detail, solutions of **1–4** (c = 2.0 mM) in DMSO-d_6 and D_2O were prepared and maintained at 37 °C for 72 h, then stability of **1–4** was monitored by ^{1}H NMR and, for PTA-containing derivatives **3** and **4**, also by ^{31}P NMR spectroscopy (Supporting Information, Figs. S6-S15).

In DMSO-d_6 and D_2O solution all Ru(II) complexes **1–4** were found to be stable toward hydrolysis. (Figs. S6-S19).

2.2. Molecular structures

The molecular structures of [Ru (curc)(dmso-S)([9]aneS_3)]Cl (**1**, Fig. 1) and [Ru(bdcurc)(dmso-S)([9]aneS_3)]Cl (**2**, Fig. 2) were confirmed by single crystal X-ray structure analysis (see SI for structure refinement parameters in Table S1 and coordination distances and angles in Table S2). The coordination environment of the ruthenium atom in **1** and **2** is very similar, with comparable bond lengths and angles (Table S2). The Ru—O distances (2.088/2.066 and 2.068/2.098 Å for complexes **1** and **2**, respectively) are similar to those observed for half-sandwich Ru-curcuminoid complexes previously reported, despite the different nature of the face-capping ligand ([9]aneS_3 vs η^6-arene) [14,16,30]. A significant elongation of the Ru–S([9]aneS_3) bond length *trans* to the dmso-S ligand (2.356 vs 2.294 and 2.298 Å in **1**; 2.343 vs 2.273, and 2.298 Å in **2**) is attributable to the greater *trans* influence of the dmso-S ligand as compared to curc and bdcurc [31,32]. The conformation of the curcuminoid ligand is instead markedly different in the two solid state structures. In **1** the curcumin ligand is highly planar (dihedral angle between the average planes through the two phenyl groups: 4.53°) while in complex **2** bdcurc is heavily non planar and distorted (dihedral angle: 47.92°). These different conformations could be related to the crystal packing, which differs considerably in the two structures. In the lattice of **1** the curcumin ligands of two neighboring

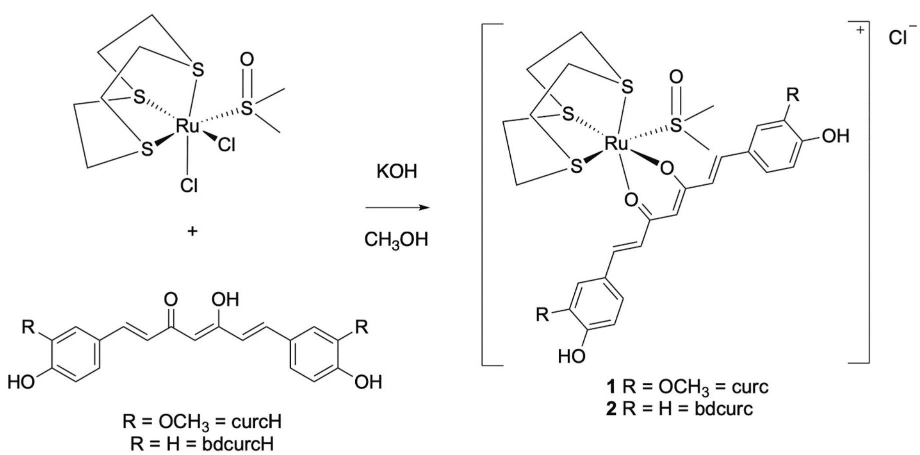

Scheme 1. Synthesis of complexes **1** and **2**.

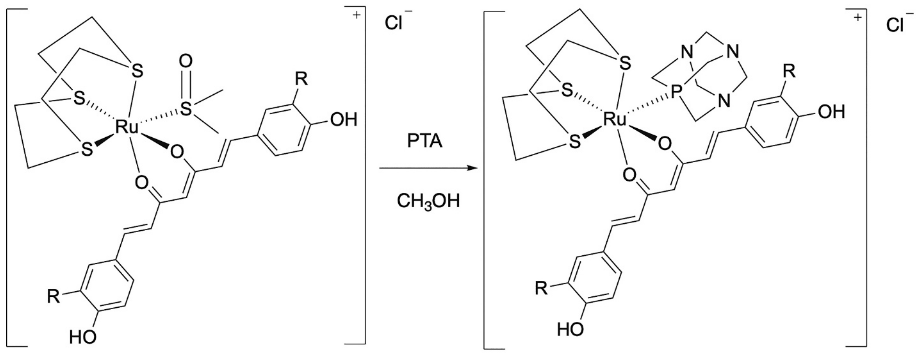

Scheme 2. Synthesis of complexes **3** and **4**.

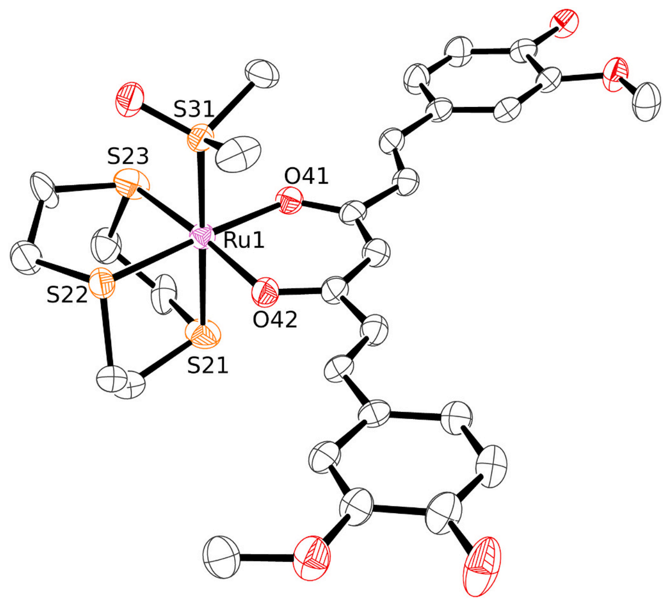

Fig. 1. ORTEP representation (50% probability ellipsoids) of the molecule of complex **1** in the crystal structure. Hydrogen atoms, two disordered water molecules and the disordered chloride anion have been omitted for clarity. Coordination distances (Å): Ru1–O41 2.088(3), Ru1–O42 2.066(3), Ru1–S21 2.356(1), Ru1–S22 2.294(1), Ru1–S23 2.298(1), Ru1–S31 2.248(1).

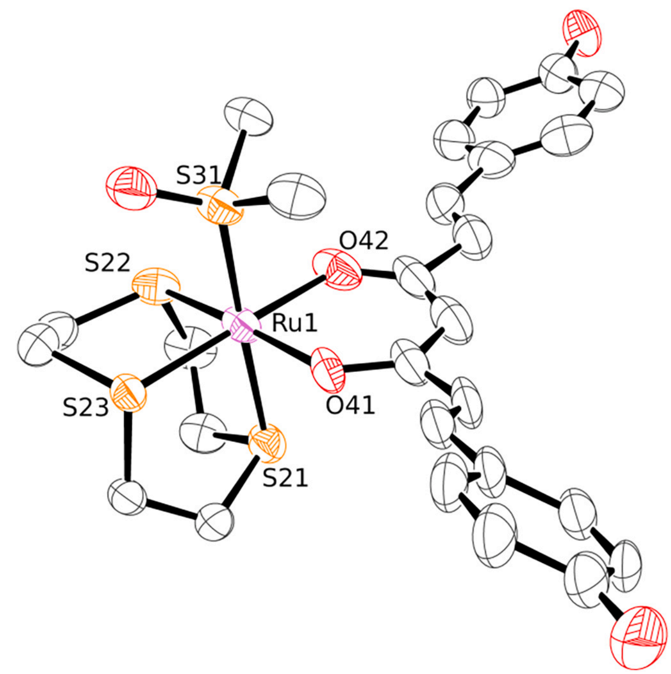

Fig. 2. ORTEP representation (50% probability ellipsoids) of the molecule of complex **2** in the crystal structure. Hydrogen atoms and the chloride anion have been omitted for clarity. Coordination distances (Å): Ru1–O41 2.068(3), Ru1–O42 2.098(3), Ru1–S21 2.343(1), Ru1–S22 2.273(1), Ru1–S23 2.298(1), Ru1–S31 2.259(1).

molecules are parallel to each other with the phenyl rings interacting via π-π stacking (centroid-centroid distance: 3.601 Å). On the other hand, in the crystal structure of **2** the bdcurc moieties of neighboring molecules are rather distant and have a non-parallel reciprocal orientation (Supporting information).

2.3. ESI MS studies of the interactions with lysozyme

Next, using a high-resolution mass spectrometry approach, we found that complexes **1**–**4** react rather modestly with hen egg white lysozyme (HEWL). This latter protein has been extensively used as model to perform bioinorganic studies aimed to characterize the activation mode of metallodrugs [33], [34] because it is cheap and possesses suitable solvent accessible aminoacidic residues e.g. His and Asp ones, capable of metal coordination [35]. Some minor differences can be detected by the comparative inspection of the recorded spectra. Indeed, complexes bearing dmso-S as ligand, i.e. **1** and **2**, show a slightly more pronounced reactivity. Specifically, **1** gives rise to different adducts characterized by the coordination of the $[Ru(curc)([9]aneS_3)]^+$ fragment with release of the dmso-S ligand (Fig. 3).

Multiple adducts were found with a stoichiometry up to 1:4 (protein to metal ratio). Additionally, the presence of a peak at 14583.7 Da assignable to the adduct with a bound $[Ru([9]aneS_3)]^{2+}$ fragment indicates the release of the curcumin ligand though in a very limited amount. In spite of this, the most intense peak is that of the native protein. At variance with **1**, compound **2** is less reactive and only a single peak falling at 14892.8 Da is detectable, that is assigned to a mono-adduct of the type $[Ru(bdcurc)([9]aneS_3)]^+$ (supporting information).

Complexes **3** and **4** are even less reactive toward HEWL. **3** coordinates the protein as demonstrated by the peak at 14952.8 Da attributable to the coordination of the fragment $[Ru(curc)([9]aneS_3)]^+$ after release of the PTA moiety. However, the intensity of this peak is very weak, while in the case of **4** no adducts formation is detectable (see supporting information).

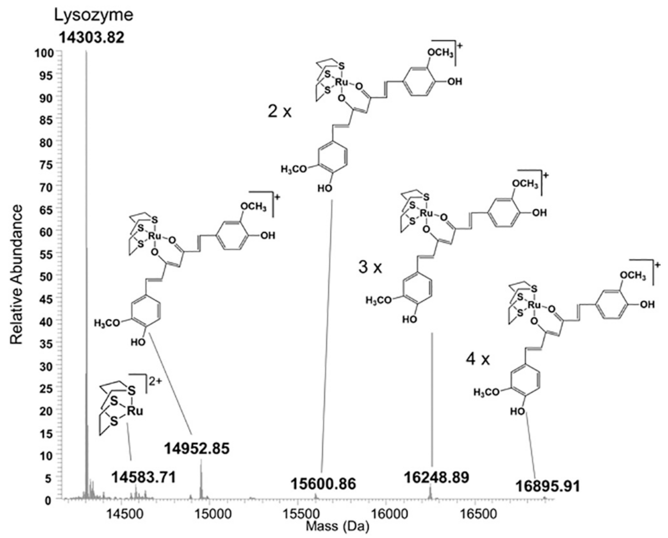

Fig. 3. Deconvoluted ESI-MS spectrum of **1** recorded after 24 h incubated at 37 °C with HEWL (10^{-4} M). Metal to protein ratio 3:1, ammonium, acetate buffer pH 6.8.

2.4. *Cellular actions*

The cytotoxic potential of the complexes **1**–**4** was evaluated against three different cancer cell lines: A549, adenocarcinoma human alveolar basal epithelial cells (NSCLC); MCF7, adenocarcinoma breast cancer cell line (ER+, PR+, HER2-) and HCT116, colorectal cancer cell line. As displayed in Table 1, curcH and bdcurcH – used as references – were able to affect significantly the A549 cell viability ($IC_{50} = 32.7 \pm 5.0$, 21.6 ± 9.8 μM, respectively) as previously reported [36,37]; conversely, the Ru complexes did not show any appreciable effect. The complexes **1**–**4** were able to slightly decrease the breast cancer cells MCF7 viability with IC_{50} values falling in the high micromolar range (Table 1). Similarly, the IC_{50} values against the colon cancer cell line HCT116 remained in the 50–200 micromolar range. The curcH and bdcurcH cytotoxic activities were in the low micromolar range in accordance with the literature data [38,39]. It is evident that coordination to the ruthenium (II) centre negatively affects the cytotoxic activity of curcH and bdcurcH. Notably, the curc complexes **1** and **3** presented a greater activity with respect to the corresponding bdcurc complexes **2** and **4**.

3. Conclusions

In this study, two cationic half-sandwich ruthenium(II) complexes [Ru(curc)(dmso-S)([9]aneS_3)]Cl (**1**) and [Ru(bdcurc)(dmso-S)([9]aneS_3)]Cl (**2**) have been prepared and characterized, both in solution and in the solid state. The corresponding PTA containing complexes [Ru(curc)(PTA)([9]aneS_3)]Cl (**3**) and [Ru(bdcurc)(PTA)([9]aneS_3)]Cl (**4**) have been also synthesized and characterized. The X-ray structures of the two Ru(II) heteroplectic complexes **1** and **2**, containing both curcumins and a face-capping ligand other than arene ones were solved for the first time. ESI MS studies were then carried out to assess the interactions of the above complexes with the model protein hen egg white lysozyme (HEWL). Overall, a rather limited reactivity with lysozyme was highlighted accompained by a generally modest cytotoxic potency against three rapresentative cancer cell lines. Consistent with previous results obtained with numerous Ru(II)-[9]aneS_3 complexes bearing a chelating nitrogen ligand (e.g. en, bpy) in the place of curcumin [27] the moderate anticancer activity in vitro may be explained on the ground of the relatively large stability of these complexes. Owing to their moderate but still measurable biolgical activity these compounds might be further explored as selective inhibitors of specific enzymatic activities.

Table 1
IC_{50} Values (μM) determined for complex **1**–**4**, curcH and bdcurcH.[a]

Complex	A549	MCF7	HCT116
1	> 500	165.9 ± 7.8	116.1 ± 18.2
2	> 500	233.7 ± 41.0	191.3 ± 11.1
3	> 500	84.7 ± 12.8	68.0 ± 7.6
4	> 500	198.7 ± 19.4	170.6 ± 47.1
curcH	32.7 ± 5.0	10.5 ± 0.4	7.1 ± 3.2
bdcurcH	21.6 ± 9.8	8.4 ± 3.3	11.5 ± 1.8

[a] Results are reported as the mean ± SD of three independent experiments.

4. Experimental

4.1. *Materials and methods*

The precursor [RuCl_2(dmso-S)([9]aneS_3)] was prepared according to literature procedures [40]. [41] The PTA was purchased from Aldrich, curcumin (curcH) and bisdemethoxycurcumin (bdcurcH) were purchased from TCI Europe and were all used as received. All other materials were obtained from commercial sources and were used as received. IR spectra were recorded from 4000 to 200 cm^{-1} on a PerkinElmer Frontier FT-IR instrument. ^{1}H, $^{13}C\{^{1}H\}$ and $^{31}P\{^{1}H\}$ NMR spectra were recorded with a 500 Bruker Ascend (500 MHz for ^{1}H, 125 MHz for ^{13}C, 202.5 MHz for ^{31}P) instrument (Bruker Corporation, Billerica, MA, USA) operating at room temperature relative to TMS. Positive ion electrospray mass spectra (ESI-MS) were obtained on a Series 1100 MSI detector HP spectrometer (Agilent Technologies, Santa Clara, CA, USA), using methanol as solvent for complexes **1**–**4**. Solutions (3 mg/mL) for electrospray ionization mass spectrometry (ESI-MS) were prepared using reagent-grade methanol. Melting points are uncorrected and were recorded on a STMP3 Stuart scientific instrument (Cole-Parmer, Stone, UK). Samples for microanalysis were dried in vacuo to constant weight (20 °C, ca. 0.1 Torr) and analysed on a Fisons Instruments 1108 CHNS-O elemental analyzer (Fisons Instruments, Ipswich, UK).

4.2. *X-ray crystallography*

Data collections were performed at the X-ray diffraction beamline (XRD1) of the Elettra Synchrotron of Trieste (Italy) equipped with a Pilatus 2 M image plate detector. Collection temperature was 100 K (nitrogen stream supplied through an Oxford Cryostream 700); the wavelength of the monochromatic X-ray beam was 0.700 Å and the diffractograms were obtained with the rotating crystal method. The crystals were dipped in N-paratone and mounted on the goniometer head with a nylon loop. The diffraction data were indexed, integrated and scaled using the XDS code [42]. The structures were solved by the dual space algorithm implemented in the SHELXT code [43]. Fourier analysis and refinement were performed by the full-matrix least-squares methods based on F2 implemented in SHELXL [44]. The Coot program was used for modelling [COOT] [45]. Anisotropic thermal motion was allowed for all non-hydrogen atoms. Hydrogen atoms were placed at calculated positions with isotropic factors $U = 1.2 \times Ueq$, where Ueq is the equivalent isotropic thermal factor of the bonded non hydrogen atom. Crystal data and details of refinements are given in the Supporting Information.

CCDC 2042166 (for **1**) and 2,042,167 (for **2**) contain the supplementary crystallographic data for this paper. These data can be obtained free of charge at www.ccdc.cam.ac.uk/conts/retrieving.html [or from the Cambridge Crystallographic Data Centre, 12, Union Road, Cambridge CB2 1EZ, UK; fax: (internat.) +44–1223/336–033; *E*-mail: deposit@ccdc.cam.ac.uk].

4.3. *Mass spectrometry studies*

A solution of each complex, (3×10^{-4} mol/L) with HEWL (3:1

complex/protein molar ratio) was incubated in ammonium acetate buffer solution 20 mM pH = 6.8 at 37 °C for 24 h and ESI MS spectra were recorded. After a 20-fold dilution with water, ESI MS spectra were recorded by direct introduction at 5 μL min^{-1} flow rate in an Orbitrap high-resolution mass spectrometer (Thermo, San Jose, CA, USA), equipped with a conventional ESI source. The working conditions were the following: spray voltage 3.1 k*V*, capillary voltage 45 V, capillary temperature 220 °C, tube lens voltage 230 V. The sheath and the auxiliary gases were set, respectively, at 17 (arbitrary units) and 1 (arbitrary units). For acquisition, Xcalibur 2.0. software (Thermo) was used and monoisotopic and average deconvoluted masses were obtained by using the integrated Xtract tool. For spectrum acquisition a nominal resolution (at *m/z* 400) of 100,000 was used.

4.4. Biological studies

4.4.1. Cell culture

Human type II alveolar epithelial cells (A549, American Type Culture Collection, CCL-195) were kindly provided by Dr. R. Danesi, University of Pisa, Pisa, Italy. Human breast cancer cells (MCF7, American Type Culture Collection, HTB-22) and human colorectal carcinoma cells (HCT116, American Type Culture CollectionCCL-247) were kindly provided by Dr. Tania Gamberi, Department of Experimental and Clinical Biomedical Sciences “Mario Serio”, University of Florence. Cells were maintained in DMEM-F12 (Cat. N. 10–092-CV, Corning) containing 10% FBS (Cat. N. 35–079-CV, Corning), 2 mM L-glutamine, 100 U/ml penicillin and 100 μg/ml streptomycin at 37 °C in a humidified 5% CO_2atmosphere. The medium was changed to remove non-adherent cells every 2–3 days.

4.5. Cell viability assay (MTS)

Cells were seeded in 96-well microplates (3.000 cells/well) and treated with different concentrations of complex **1**–**4**, curcH and bdcurcH (1 μM to 250 μM). The final DMSO concentration was 1%. Following the treatment period, cell viability was determined using an MTS assay (CellTiter 96 AQueous One Solution Cell Proliferation Assay kit; Promega, Milan, Italy) according to the manufacturer’s instructions. The absorbance at 490 nm was measured with the EnSightTM multimode plate reader (Perkin Elmer, Waltham, MA, USA). Three independent experiments were performed in duplicate. The percentage of cell viability were calculated respect to control cells treated with the same amount of DMSO.

4.6. Statistical analysis

Graph-Pad Prism 6.0 (GraphPad Software Inc., San Diego, CA) was used for data analysis and graphic presentations. The IC_{50} values were calculated using the non-linear fit log(inhibitor) vs. normalized response – Variable slope.

4.7. Syntheses and characterization

4.7.1. [Ru(curc)(dmso-S)([9]aneS_3)]Cl (1)

Curcumin (280 mg, 0.76 mmol) was dissolved in methanol (20 mL) and CH_3ONa (40.0 mg, 0.76 mmol) was added. The mixture was stirred for 1 h at room temperature and then [RuCl_2(dmso-S)([9]aneS_3)] (328 mg, 0.76 mmol) was added. The mixture was stirred under reflux for 5 h and then 24 h at room temperature. The solvent was removed under reduced pressure and dichloromethane (10 mL) was added and the mixture was filtered to remove sodium chloride. The solution was concentrated to ca. 2 mL and stored at 4 °C affording orange crystals (160 mg, 0.208 mmol, yield 27%). Compound **1** is soluble in alcohols, dmso, DMF, water and partially soluble in chlorinated solvents, acetonitrile and acetone. Crystals of **1** suitable for X-ray diffraction were grown from a 3/1 mixture of dichloromethane and n-hexane. Mp: 194 °C. Anal. Calcd for $C_{29}H_{37}ClO_7RuS_4$: C, 45.69; H, 4.89; S, 16.82. Found: C, 45.56; H, 4.79; S, 16.68. Λ_m (dmso, 293 K, 10^{-4} mol/L): 38 S cm^2 mol^{-1}. IR (cm^{-1}): 3009mbr, 1617 m, 1593 m, 1582 m and 1491s ν(C=C; C=O), 1393 m, 1271s, 1162s, 1123s, 1079s ν(S=O_{dmso-S}), 966 m, 834 m, 805 m, 681 s, 558 s, 450 w, 424 s ν(Ru–S_{dmso-S}), 389 s. ^{1}H NMR (DMSO-d_6, 293 K): δ, 2.66–2.92 (m, 12H, C*H*$_2$[9]aneS_3), 3.81 (s, 6H, OC*H*$_3$ of curc), 5.83 (s, 1H, C(1)*H* of curc), 6.71 (d, 2H, C(4, 4’)*H* of curc), 6.78 (d, 2H, C(10, 10’)*H* of curc), 7.08 (d, 2H, C(9, 9’)*H* of curc), 7.24 (s, 2H, C(6, 6’)*H* of curc), 7.31 (d, 2H, C(3, 3’)*H* of curc), 9.57 (br, 2H, O*H* of curc). ^{13}C{^{1}H} NMR (DMSO-d_6, 293 K): δ, 30.6, 33.1, 35.1 (s, *C*H_2 [9]aneS_3), 41.1, 43.3 (s, CH_3), 56.7 (s, OCH_3 of curc), 102.3 (s, *C*(1) of curc), 111.6 (s, *C*(6, 6′) of curc), 116.3 (s, *C*(9, 9′) of curc), 122.9 (s, *C* (10, 10′) of curc), 125.9 (s, *C*(5, 5′) of curc), 127.6 (s, *C*(3, 3′) of curc), 139.1 (s, *C*(4, 4′) of curc), 148.6 (s, *C*(7, 7′) of curc), 149.3 (s, *C*(8, 8′) of curc), 179.9 (s, *C*(2, 2′) = O of curc). ESI-MS (+) CH_3OH (*m/z*, relative intensity %): 727 [100], [Ru(curc)(dmso-S)([9]aneS_3)]$^+$, 649 [10], [Ru (curc)([9]aneS_3)]$^+$.

4.7.2. [Ru(bdcurc)(dmso-S)([9]aneS_3)]Cl (2)

To the bisdemethoxycurcumin (bdcurcH, 234 mg, 0.76 mmol) dissolved in methanol (20 mL), CH_3ONa (40.0 mg, 0.76 mmol) was added. The mixture was stirred for 1 h at room temperature and then [RuCl_2(dmso-S)([9]aneS_3)] (328 mg, 0.76 mmol) was added. The resulting solution was stirred under reflux for 5 h and then 24 h at room temperature. The solvent was removed under reduced pressure and dichloromethane (10 mL) was added and the mixture was filtered to remove sodium chloride. The solution was concentrated to ca. 2 mL and stored at 4 °C affording orange crystals (140 mg, 0.199 mmol, yield 26%.). Compound **2** is soluble in alcohols, DMSO, DMF, water and partially soluble in chlorinated solvents, acetonitrile and acetone. Crystals of **2** suitable for X-ray diffraction were grown from a 3/1 mixture of dichloromethane and n-hexane. Mp: 206 °C. Anal. Calcd for $C_{27}H_{33}ClO_5RuS_4$: C, 46.18; H, 4.74; S, 18.26. Found: C, 46.06; H, 4.69; S, 18.09. Λ_m (DMSO, 293 K, 10^{-4} mol/L): 37 S cm^2 mol^{-1}. IR (cm^{-1}): 3118mbr, 1621 m, 1600 m and 1500sν (C=C; C=O), 1421 m, 1393 m, 1270 m, 1165s, 1069 m ν(S=O_{dmso-S}), 983 m, 834 m, 681 s, 551 s, 522 s, 487 s, 456 m, 425 s (Ru—S), 390 s. ^{1}H NMR (DMSO-d_6, 293 K): δ, 2.63–2.89 (m, 12H, C*H*$_2$[9]aneS_3), 5.78 (s, 1H, C(1)*H* of bdcurc), 6.63 (d, 2H, C(4, 4’)*H* of bdcurc), 6.77 (d, 4H, C(6, 6’)*H* e C(10, 10’)*H* of bdcurc), 7.30 (d, 2H, C(3, 3’)*H* of bdcurc), 7.48 (d, 4H, C(7, 7’)*H*e C(9, 9’)*H* of bdcurc), 9.97 (br, 2H, O*H* of bdcurc). ^{13}C{^{1}H} NMR (DMSO-d_6, 293 K): δ, 30.7, 31.5, 33.1, 34.5, 34.9, 35.1 (s, CH_2[9]aneS_3), 43.3, 44.5 (s, *C*H_3), 103.4 (s, *C*(1) of bdcurc), 116.5 (s, *C*(6, 6′) e *C*(10, 10′) of bdcurc), 125.6 (s, *C*(5, 5′) of bdcurc), 127.1 (s, *C*(3, 3′) of bdcurc), 130.4 (s, *C*(7, 7′) e *C*(9, 9′) of bdcurc), 138.9 (s, *C*(4, 4′) of bdcurc), 159.8 (s, *C* (8, 8′) of bdcurc), 179.8 (s, *C*(2, 2′) = O of bdcurc). ESI-MS (+) CH_3OH (*m/z*, relative intensity %): 667 [100], [Ru(bdcurc)(dmso-S)([9] aneS^3)]$^+$, 588 [10], [Ru(bdcurc)([9]aneS^3)]$^+$.

4.7.3. [Ru(curc)(PTA)([9]aneS_3)]Cl (3)

Compound **1** (100 mg, 0.131 mmol) was dissolved in methanol (10 mL) and PTA (20.6 mg, 0.131 mmol) was added. The mixture was stirred for 24 h at room temperature. Then the solution was dried by rotary evaporation and dichloromethane (2 mL) and an excess of *n*-hexane were added. The mixture was left at 4 °C until a yellow precipitate formed. The powder was recovered by filtration and air-dried. Compound **3** (38.6 mg, 0.046 mmol, yield 35%), is soluble in alcohols, acetone, acetonitrile, chlorinated solvents, DMF, DMSO and water. Mp: 219–221 °C. Anal. Calcd for $C_{33}H_{43}ClN_3O_6PRuS_3$: C, 47.11; H, 5.15; N, 4.99; S, 11.43. Found: C, 46.97; H, 5.07; N, 4.85; S, 11.30. Λ_m (DMSO, 293 K, 10^{-4} mol/L): 40 S cm^2 mol^{-1}. IR (cm^{-1}): 3356mbr, 1621 m, 1588 m and 1503s ν(C=C; C=O), 1402 m, 1279 m, 1239 m, 1160 m, 1124 m, 1012 m, 969 m, 948 m, 808 m, 742 m, 574 m, 478 m, 451 m, 397 m. ^{1}H NMR (DMSO-d_6, 293 K): δ, 2.49–2.91 (m, 12H, C*H*$_2$ [9] aneS_3), 3.81 (s, 6H, OC*H*$_3$ di curc), 3.96 (s, 6H, P-C*H*$_2$-N, PTA), 4.39 (s, 6H, N-C*H*$_2$-N, PTA), 5.80 (s, 1H, C(1)*H* of curc), 6.65 (d, 2H, C(4, 4’)*H* of curc), 6.78 (d, 2H, C(10, 10')*H* of curc), 7.06 (d, 2H, C(9, 9')*H* of curc), 7.19 (d, 2H, C(3, 3')*H* of curc), 7.22 (s, 2H, C(6, 6')*H* of curc), 9.51 (s, 2H, O*H* of curc). $^{13}C\{^1H\}$ NMR (DMSO-d_6, 293 K): δ, 30.4, 33.1, 34.9 (s, CH_2 [9]aneS_3), 54.2 (d, PCH_2N, PTA), 56.8 (s, OCH_3 of curc), 76.3 (d, NCH_2N, PTA), 104.3 (s, *C*(1) of curc), 112.9 (s, *C*(6, 6′) of curc), 118.1 (s, *C*(9, 9′) of curc), 125.4 (s, *C*(10, 10′) of curc), 126.8 (s, *C*(5, 5′) of curc), 127.5 (s, *C*(3, 3′) of curc), 140.3 (s, *C*(4, 4′) of curc), 149.9 (s, *C*(7, 7′) of curc), 151.2 (s, *C*(8, 8′) of curc), 181.2 (s, *C*(2, 2′) = O of curc).$^{31}P\{^1H\}$ NMR (DMSO-d_6, 298 K): $\delta = -28.7$ ESI-MS (+) CH_3OH (*m/z*, relative intensity %): 806 [100][Ru(curc)(PTA)([9]aneS_3)]$^+$.

4.7.4. [Ru(bdcurc)(PTA)[([9]aneS$_3$)]Cl (4)

Compound **2** (100 mg, 0.142 mmol) was dissolved in methanol (10 mL) and PTA (22.3 mg, 0.142 mmol) was added. The mixture was stirred for 24 h at room temperature. Then the solution was dried by rotary evaporation and dichloromethane (2 mL) and an excess of *n*-hexane were added. The mixture was left at 4 °C until a yellow precipitate formed. The powder was recovered by filtration and air-dried. Compound **4** (37.7 mg, 0.048 mmol, yield 34%) is soluble in alcohols, acetone, acetonitrile, chlorinated solvents, DMF, DMSO and water. Mp: 237–238 °C. Anal. Calcd for $C_{31}H_{39}ClN_3O_4PRuS_3$: C, 47.65; H, 5.03; N, 5.38; S, 12.31. Found: C, 47.21; H, 4.91; N, 5.31; S, 12.23. Λ_m (DMSO, 293 K, 10^{-4} mol/L): 38 S cm^2 mol^{-1}. IR (cm^{-1}): 2933mbr, 1622 m, 1602 m, 1580 m and 1500sν (C=C; C=O), 1401 m, 1277 m, 1238 m, 1163s, 1100 m, 1012 m, 966 s, 947 s, 826 m, 741 m, 689 m, 599 m, 575 s, 548 m, 517 s, 481 s, 451 m, 391 m, 381 m, 336 m. ^1H NMR (DMSO-d_6, 293 K): δ, 2.52–2.89 (m, 12H, CH_2[9]aneS_3), 3.95 (s, 6H, P-CH_2-N, PTA), 4.37 (s, 6H, N-CH_2-N, PTA), 5.75 (s, 1H, C(1)*H* of bdcurc), 6.59 (d, 2H, C(4, 4')*H* of bdcurc), 6.77 (d, 4H, C(6, 6')*H* e C(10, 10')*H* of bdcurc), 7.17 (d, 2H, C(3, 3')*H* of bdcurc), 7.46 (d, 4H, C(7, 7')*H*e C(9, 9')*H* of bdcurc), 9.96 (br, 2H, O*H* of bdcurc). $^{13}C\{^1H\}$ NMR (DMSO-d_6, 293 K): δ, 33.5, 38.7, 42.7 (s, CH_2[9]aneS_3), 55.8 (d, P-CH_2-N, PTA), 77.4 (d, N-CH_2-N, PTA), 107.9 (s, *C*(1) of bdcurc), 121.2 (s, *C*(6, 6′) e *C* (10, 10′) of bdcurc), 130.6 (s, *C*(5, 5′) of bdcurc), 131.9 (s, *C*(3, 3′) of bdcurc), 134.9 (s, *C*(7, 7′) e *C*(9, 9′) of bdcurc), 142.6 (s, *C*(4, 4′) of bdcurc), 164.3 (s, *C*(8, 8′) of bdcurc), 184.4 (s, *C*(2, 2′) = O of bdcurc).).$^{31}P\{^1H\}$ NMR (DMSO-d_6, 298 K): $\delta = -28.7$. ESI-MS (+) CH_3OH (*m/z*, relative intensity %): 746 [100][Ru(bdcurc)(PTA) ([9] aneS^3)]$^+$.

Declaration of competing Interest

There are no conflicts to declare.

Acknowledgements

We thank the University of Camerino for financial support. LM and TM thank Ente Cassa Risparmio Firenze (ECR), and AIRC for funding the project "Advanced mass spectrometry tools for cancer research: novel applications in proteomics, metabolomics and nanomedicine" (Multi-user Equipment Program 2016, Ref. code 19650) and the Beneficentia Stiftung, Vaduz. TM, CG, LMa, MT and DM thank University of Pisa (Rating Ateneo 2019-2020) for the financial support. This work is also supported by the University of Pisa under the "PRA – Progetti di Ricerca di Ateneo" Institutional Research Grants – Project no. PRA_2020_58 "Agenti innovativi e nanosistemi per target molecolari nell'ambito dell'oncologia di precisione" to TM and DM. The CIRCMSB, Bari is also acknowledged.

References

[1] B.B. Aggarwal, C. Sundaram, N. Malani, H. Ichikawa, Curcumin: the Indian solid gold, in: Mol. Targets Ther. Uses Curcumin Heal. Dis, Springer, 2007, pp. 1–75.
[2] B. Salehi, Z. Stojanović-Radić, J. Matejić, M. Sharifi-Rad, N.V. Anil Kumar, N. Martins, J. Sharifi-Rad, The therapeutic potential of curcumin: a review of clinical trials, Eur. J. Med. Chem. 163 (2019) 527–545.
[3] W. Liu, Y. Zhai, X. Heng, F.Y. Che, W. Chen, D. Sun, G. Zhai, Oral bioavailability of curcumin: problems and advancements, J. Drug Target. 24 (2016) 694–702.
[4] S. Wanninger, V. Lorenz, A. Subhan, F.T. Edelmann, Metal complexes of curcumin - synthetic strategies, structures and medicinal applications, Chem. Soc. Rev. 44 (2015) 4986–5002.
[5] A. Shakeri, Y. Panahi, T.P. Johnston, A. Sahebkar, Biological properties of metal complexes of curcumin, BioFactors 45 (2019) 304–317.
[6] F. Kühlwein, K. Polborn, W. Beck, Metallkomplexe von Farbstoffen. VIII Übergangsmetallkomplexe des Curcumins und seiner Derivate, Zeitschrift Für Anorg. Und Allg. Chem. 623 (1997) 1211–1219.
[7] P. Srivastava, M. Shukla, G. Kaul, S. Chopra, A.K. Patra, Rationally designed curcumin based ruthenium(II) antimicrobials effective against drug-resistant: staphylococcus aureus, Dalton Trans. 48 (2019) 11822–11828.
[8] D. Pucci, T. Bellini, A. Crispini, I. D'Agnano, P.F. Liguori, P. Garcia-Orduña, S. Pirillo, A. Valentini, G. Zanchetta, DNA binding and cytotoxicity of fluorescent curcumin-based Zn(II) complexes, Medchemcomm 3 (2012) 462–468.
[9] A. Hussain, K. Somyajit, B. Banik, S. Banerjee, G. Nagaraju, A.R. Chakravarty, Enhancing the photocytotoxic potential of curcumin on terpyridyl lanthanide(III) complex formation, Dalton Trans. 42 (2013) 182–195.
[10] T. Sarkar, S. Banerjee, S. Mukherjee, A. Hussain, Mitochondrial selectivity and remarkable photocytotoxicity of a ferrocenyl neodymium(III) complex of terpyridine and curcumin in cancer cells, Dalton Trans. 45 (2016) 6424–6438.
[11] C. Triantis, T. Tsotakos, C. Tsoukalas, M. Sagnou, C. Raptopoulou, A. Terzis, V. Psycharis, M. Pelecanou, I. Pirmettis, M. Papadopoulos, Synthesis and characterization of fac-[M(CO)$_3$(P)(OO)] and cis-trans-[M(CO)$_2$(P)$_2$(OO)] complexes (M = Re, ^{99}mTc) with acetylacetone and curcumin as O,O donor bidentate ligands, Inorg. Chem. 52 (2013) 12995–13003.
[12] R. Pettinari, F. Marchetti, C. Pettinari, F. Condello, A. Petrini, R. Scopelliti, T. Riedel, P.J. Dyson, Organometallic rhodium(III) and iridium(III) cyclopentadienyl complexes with curcumin and bisdemethoxycurcumin co-ligands, Dalton Trans. 44 (2015) 20523–20531.
[13] R. Pettinari, F. Marchetti, C. Di Nicola, C. Pettinari, M. Cuccioloni, L. Bonfili, A. M. Eleuteri, B. Therrien, L.K. Batchelor, P.J. Dyson, Novel osmium(ii)-cymene complexes containing curcumin and bisdemethoxycurcumin ligands, Inorg. Chem. Front. 6 (2019) 2448–2457.
[14] R. Pettinari, F. Marchetti, F. Condello, C. Pettinari, G. Lupidi, R. Scopelliti, S. Mukhopadhyay, T. Riedel, P.J. Dyson, Ruthenium(II)-arene RAPTA type complexes containing curcumin and bisdemethoxycurcumin display potent and selective anticancer activity, Organometallics 33 (2014) 3709–3715.
[15] F. Caruso, M. Rossi, A. Benson, C. Opazo, D. Freedman, E. Monti, M.B. Gariboldi, J. Shaulky, F. Marchetti, R. Pettinari, C. Pettinari, Ruthenium-arene complexes of curcumin: X-ray and density functional theory structure, synthesis, and spectroscopic characterization, in vitro antitumor activity, and DNA docking studies of (p-cymene)Ru(curcuminato)chloro, J. Med. Chem. 55 (2012) 1072–1081.
[16] R. Pettinari, A. Petrini, F. Marchetti, C. Di Nicola, R. Scopelliti, T. Riedel, L. D. Pittet, A. Galindo, P.J. Dyson, Influence of functionalized η6-arene rings on ruthenium(II) curcuminoids complexes, ChemistrySelect. 3 (2018) 6696–6700.
[17] Z. Mendoza, P. Lorenzo-Luis, M. Serrano-Ruiz, E. Martín-Batista, J.M. Padrón, F. Scalambra, A. Romerosa, Synthesis and antiproliferative activity of [RuCp (PPh$_3$)$_2$(HdmoPTA)](OSO$_2$CF$_3$)$_2$ (HdmoPTA = 3,7-H-3,7-dimethyl-1,3,7-triaza-5 phosphabicyclo[3.3.1]nonane), Inorg. Chem. 55 (2016) 7820–7822.
[18] Z. Mendoza, P. Lorenzo-Luis, F. Scalambra, J.M. Padrón, A. Romerosa, Enhancement of the antiproliferative activity of [RuCp(PPh$_3$)$_2$(dmoPTA-1κP)]$^+$ via its coordination to one {CoCl$_2$} unit: synthesis crystal structure and properties of [RuCp(PPh$_3$)$_2$-μ-dmoPTA-1κP:2κ^{2}N,N′-CoCl$_2$](OTf)·0.25H$_2$O, Dalton Trans. 46 (2017) 8009–8012.
[19] Z. Mendoza, P. Lorenzo-Luis, F. Scalambra, J.M. Padrón, A. Romerosa, One step up in antiproliferative activity: the Ru-Zn complex [RuCp(PPh$_3$)$_2$-μ-dmoPTA-1κP: 2κ^{2}N,N′-ZnCl$_2$](CF$_3$SO$_3$), Eur. J. Inorg. Chem. 2018 (2018) 4684–4688.
[20] S. Huang, J. Xie, W. Su, Y. Liu, X. Wang, B. Hu, Q. Xiao, Comparative investigation of interactions between two ruthenium(II) arene PTA type complexes with curcuminoid ligands and human serum albumin, J. Organomet. Chem. 853 (2017) 81–92.
[21] S. Huang, H. Li, Y. Liu, Y. Liang, W. Su, Q. Xiao, Comparable investigation of in vitro interactions between three ruthenium(II) arene complexes with curcumin analogs and ctDNA, Polyhedron 167 (2019) 51–61.
[22] B. Serli, E. Zangrando, T. Gianferrara, C. Scolaro, P. Dyson, A. Bergamo, E. Alessio, Is the aromatic fragment of piano stool ruthenium compounds an essential feature for anticancer activity? The development of new RuIO-[9]aneS3 analogues, Eur. J. Inorg. Chem. 2005 (2005) 3423–3434.
[23] I. Bratsos, G. Birarda, S. Jedner, E. Zangrando, E. Alessio, Half-sandwich RuII-[9] aneS$_3$ complexes with dicarboxylate ligands: synthesis, characterization and chemical behavior, Dalton Trans. (2007) 4048–4058.
[24] I. Bratsos, S. Jedner, A. Bergamo, G. Sava, T. Gianferrara, E. Zangrando, E. Alessio, Half-sandwich RuII[9]aneS3 complexes structurally similar to antitumor-active organometallic piano-stool compounds: preparation, structural characterization and in vitro cytotoxic activity, J. Inorg. Biochem. 102 (2008) 1120–1133.

[25] A. Rilak, I. Bratsos, E. Zangrando, J. Kljun, I. Turel, Ž.D. Bugarčić, E. Alessio, Factors that influence the antiproliferative activity of half sandwich RuII–[9]aneS_3 coordination compounds: activation kinetics and interaction with guanine derivatives, Dalton Trans. 41 (2012) 11608–11618.
[26] G. Ragazzon, I. Bratsos, E. Alessio, L. Salassa, A. Habtemariam, R.J. McQuitty, G. J. Clarkson, P.J. Sadler, Design of photoactivatable metallodrugs: selective and rapid light-induced ligand dissociation from half-sandwich [Ru([9]aneS_3)(N–N′)(py)]$^{2+}$ complexes, Inorg. Chim. Acta 393 (2012) 230–238.
[27] A. Rilak Simović, R. Masnikosa, I. Bratsos, E. Alessio, Chemistry and reactivity of ruthenium(II) complexes: DNA/protein binding mode and anticancer activity are related to the complex structure, Coord. Chem. Rev. 398 (2019) 113011.
[28] M.C. Henriques, M.A.F. Faustino, A.M.S. Silva, J. Felgueiras, M. Fardilha, S. S. Braga, A ruthenium(II)-trithiacyclononane curcuminate complex: synthesis, characterization, DNA-interaction, and cytotoxic activity, J. Coord. Chem. 70 (2017) 2393–2408.
[29] F. Battistin, A. Vidal, G. Balducci, E. Alessio, Investigating the reactivity of neutral water-soluble Ru(II)–PTA carbonyls towards the model imine ligands pyridine and 2,2′-bipyridine, RSC Adv. 10 (2020) 26717–26727.
[30] R. Pettinari, F. Marchetti, C. Pettinari, P. Smoleński, T. Riedel, R. Scopelliti, P. J. Dyson, Dicationic ruthenium(II)arene–curcumin complexes containing methylated 1,3,5-Triaza-7-phosphaadamantane: synthesis, structure, and cytotoxicity, Eur. J. Inorg. Chem. (2017) 2905–2910.
[31] E. Alessio, Synthesis and reactivity of Ru-, Os-, Rh-, and Ir-halide−sulfoxide complexes, Chem. Rev. 104 (2004) 4203–4242.
[32] I. Bratsos, E. Alessio, The pivotal role of Ru-dmso compounds in the discovery of well-behaved precursors, Eur. J. Inorg. Chem. 2018 (2018) 2996–3013.
[33] A. Merlino, T. Marzo, L. Messori, Protein Metalation by anticancer Metallodrugs: a joint ESI MS and XRD investigative strategy, Chem. – A Eur. J. 23 (2017) 6942–6947.
[34] D. Cirri, S. Pillozzi, C. Gabbiani, J. Tricomi, G. Bartoli, M. Stefanini, E. Michelucci, A. Arcangeli, L. Messori, T. Marzo, PtI2(DACH){,} the iodido analogue of oxaliplatin as a candidate for colorectal cancer treatment: chemical and biological features, Dalton Trans. 46 (2017) 3311–3317.
[35] L. Messori, T. Marzo, A. Merlino, The X-ray structure of the complex formed in the reaction between oxaliplatin and lysozyme, Chem. Commun. 50 (2014) 8360–8362.
[36] S. Jayakumar, R.S. Patwardhan, D. Pal, D. Sharma, S.K. Sandur, Dimethoxycurcumin, a metabolically stable analogue of curcumin enhances the radiosensitivity of cancer cells: possible involvement of ROS and thioredoxin reductase, Biochem. Biophys. Res. Commun. 478 (2016) 446–454.
[37] D. Tunc, E. Dere, D. Karakas, B. Cevatemre, V.T. Yilmaz, E. Ulukaya, Cytotoxic and apoptotic effects of the combination of palladium (II) 5,5-diethylbarbiturate complex with bis(2-pyridylmethyl)amine and curcumin on non small lung cancer cell lines, Bioorg. Med. Chem. 25 (2017) 1717–1723.
[38] M. Shakibaei, A. Mobasheri, C. Lueders, F. Busch, P. Shayan, A. Goel, Curcumin enhances the effect of chemotherapy against colorectal cancer cells by inhibition of NF-κB and Src protein kinase signaling pathways, PLoS One 8 (2013) e57218.
[39] M.J. Yoon, Y.J. Kang, J.A. Lee, I.Y. Kim, M.A. Kim, Y.S. Lee, J.H. Park, B.Y. Lee, I. A. Kim, H.S. Kim, S.-A. Kim, A.-R. Yoon, C.-O. Yun, E.-Y. Kim, K. Lee, K.S. Choi, Stronger proteasomal inhibition and higher CHOP induction are responsible for more effective induction of paraptosis by dimethoxycurcumin than curcumin, Cell Death Dis. 5 (2014) e1112.
[40] C. Landgrafe, W.S. Sheldrick, Structure and reactions of the thioether half-sandwich ruthenium(II) complexes [Ru(MeCN)3([9]aneS3)][CF3SO3]2 and [Ru(MeCN)2(PPh3)([9]aneS3)][CF3SO3]2([9]aneS3= 1,4,7-trithiacyclononane), J. Chem. Soc. Dalton Trans. (1994) 1885–1893.
[41] K. Brandt, W.S. Sheldrick, Synthesis{,} structure and reactivity of the thioether half-sandwich rhodium(III) complex [RhCl(MeCN)2([9]aneS3)][CF3SO3]2([9]aneS3= 1,4,7-trithiacyclononane), J. Chem. Soc. Dalton Trans. (1996) 1237–1243.
[42] W. Kabsch, W. XDS, Acta Crystallogr. Sect. D 66 (2010) 125–132.
[43] G.M. Sheldrick, SHELXT - integrated space-group and crystal-structure determination, Acta Crystallogr. Sect. A. 71 (2015) 3–8.
[44] G.M. Sheldrick, A short history of SHELX, Acta Crystallogr. Sect. A. 64 (2008) 112–122.
[45] P. Emsley, K. Cowtan, Coot: model-building tools for molecular graphics, Acta Crystallogr. Sect. D 60 (2004) 2126–2132.